

Title:

Plasticity of meiotic recombination rates in response to temperature in *Arabidopsis*

Andrew Lloyd^{1, #}, Chris Morgan^{2, 3, #}, Chris Franklin³ & Kirsten Bomblies²

¹ Institut Jean-Pierre Bourgin, INRA, AgroParisTech, CNRS, Université Paris-Saclay, RD10, 78000 Versailles, France

² John Innes Centre, Department of Cell & Developmental Biology, Norwich NR4 7UH, UK

³ School of Biosciences, University of Birmingham, Edgbaston, Birmingham B15 2TT, United Kingdom

#Co-first authors

Corresponding authors: Kirsten Bomblies, Kirsten.Bomblies@jic.ac.uk; Andrew Lloyd, andrewhmlloyd@gmail.com

Running title: Temperature affects class I crossovers

Keywords: Recombination, Crossover plasticity, Recombination rate, Temperature, meiosis

Corresponding Author:

Kirsten Bomblies

John Innes Centre

Norwich Research Park

Colney Lane

Norwich NR4 7UH

United Kingdom

Phone: +44 1603 450000 x2691

Email: Kirsten.Bomblies@jic.ac.uk

ABSTRACT

1
2 Meiotic recombination shuffles genetic information from sexual species into gametes to
3 create novel combinations in offspring. Thus, recombination is an important factor in
4 inheritance, adaptation and responses to selection. However, recombination is not a static
5 parameter; meiotic recombination rate is sensitive to variation in the environment, especially
6 temperature. That recombination rates change in response to both increases and decreases
7 in temperature was reported in *Drosophila* a century ago, and since then in several other
8 species. But it is still unclear what the underlying mechanism is, and whether low and high
9 temperature effects are mechanistically equivalent. Here we show that, as in *Drosophila*,
10 both high and low temperatures increase meiotic crossovers in *Arabidopsis thaliana*. We
11 show that, from a nadir at 18C, both lower and higher temperatures increase recombination
12 through additional class I – interfering – crossovers. The increase in crossovers at high and
13 low temperatures however appears to be mechanistically at least somewhat distinct, as they
14 differ in their association with the DNA repair protein MLH1. We also find that, in contrast
15 to what has been reported in barley, synaptonemal complex length is negatively correlated
16 with temperature; thus, an increase in chromosome axis length may account for increased
17 crossovers at low temperature in *A. thaliana*, but cannot explain the increased crossovers
18 observed at high temperature. The plasticity of recombination has important implications
19 for evolution and breeding, and also for interpreting observations of recombination rate
20 variation among natural populations.

INTRODUCTION

21
22
23
24 The vast majority of eukaryotes rely on meiosis to produce gametes. One important process
25 within meiosis is the crossing over of homologous chromosomes, which in most eukaryotes
26 is essential for stable chromosome segregation (Zickler and Kleckner 1999). Recombination
27 also shuffles the genetic complements of the two parents of an individual and is thus
28 important in generating novel genetic combinations in gametes and ultimately offspring.
29 The extent and pattern of genetic reshuffling via homologous recombination has important
30 implications for evolution and adaptation, as well as population genetics and breeding (e.g.:
31 Barton 1995; Charlesworth and Barton 1996; Otto 2009; Campos *et al.* 2015).
32 Recombination is not a static parameter between, or even within taxa. Meiotic
33 recombination rate is known to be sensitive to a variety of environmental factors,
34 particularly temperature (Plough 1917; Elliott 1955; De Storme and Geelen 2014; Bomblies

35 *et al.* 2015; Modliszewski and Copenhaver 2015; Phillips *et al.* 2015). Extreme temperatures
36 can cause meiotic recombination to fail outright due to structural disruptions of e.g. the
37 spindle, the chromosome axes, or the synaptonemal complex (Bilgir *et al.* 2013; Bomblies
38 *et al.* 2015; Morgan *et al.* 2017). We refer to the temperatures at which such defects become
39 cytologically evident as “failure thresholds.” Less extreme temperature fluctuations that do
40 not cause outright failures, can nevertheless affect the genome-wide recombination rate in
41 diverse taxa (Plough 1917; Elliott 1955; De Storme and Geelen 2014; Bomblies *et al.* 2015;
42 Modliszewski and Copenhaver 2015; Phillips *et al.* 2015). Understanding the nature and
43 strength of these effects has important implications for better understanding and predicting
44 inheritance and evolution, especially in a time of climate change, and also for managing
45 breeding programs. Understanding the effect of temperature on recombination also provides
46 opportunities to manipulate recombination in a targeted and reversible way (e.g. Phillips *et*
47 *al.* 2015).

48

49 That both temperature increases and decreases can affect meiotic recombination rates has
50 been recognized for 100 years (Plough 1917). The first investigation into the effect of
51 temperature on meiotic recombination rate suggested a U-shaped response in *Drosophila*
52 (Plough 1917; Smith 1936), meaning that mid-range temperatures (which at least in the case
53 of *Drosophila* correspond to common rearing temperatures) have the lowest recombination
54 rate, and both increases and decreases in rearing temperature are associated with elevated
55 recombination. Since the original discoveries, a variety of trends have been reported,
56 including no effect, increases with increasing temperature, and decreases with increasing
57 temperature (Elliott 1955; Stern 1926; Jensen 1981; Francis *et al.* 2007; Phillips *et al.* 2015),
58 reviewed in (Bomblies *et al.* 2015). We and others have previously suggested that while
59 there may well be biological differences among taxa, distinct reported trends can also result
60 from differences in experimental design (Wilson 1959; Bomblies *et al.* 2015), e.g. from only
61 sampling a sub-section of the relevant temperature range, or by including temperatures
62 beyond the meiotic failure limits where recombination declines sharply. Many species
63 appear to have U-shaped curves (Wilson 1959; Bomblies *et al.* 2015), but it has remained
64 unknown whether the low and high temperature effects are mechanistically distinct.

65

66 An important aspect of understanding the effects of temperature on recombination is to know
67 what type of crossovers are responsible, as this has important implications for the patterning
68 that may result. Crossovers come in two major classes. Class I crossovers represent the

69 majority of crossovers in most species (Lynn *et al.* 2007). These crossovers rely on a class
70 of proteins called ZMM proteins (Börner *et al.* 2004; Lynn *et al.* 2007; Mercier *et al.* 2014),
71 and are subject to crossover interference. Crossover interference deters crossovers from
72 forming in close proximity, and thus causes recombination events to be more widely spaced
73 than expected if they occurred randomly (Berchowitz and Copenhaver 2010). A second class
74 are called the class II crossovers. These occur through a variety of pathways but share the
75 important property that they are not subject to crossover interference and can be spaced
76 randomly (Lynn *et al.* 2007; Higgins *et al.* 2012). In most species, it is not known whether
77 temperature affects one or the other type of crossover preferentially. In barley, where
78 temperature causes a change in the positioning of crossovers to more proximal locations
79 (Higgins *et al.* 2012; Phillips *et al.* 2015), immunological staining suggests that class I
80 crossovers are affected. In yeast, temperature also has effects on ZMM-dependent (class I)
81 crossover designation (Börner *et al.* 2004). Whether temperature effects operate primarily
82 through altering class I or class II crossovers has implications for crossover positioning and
83 spacing.

84

85 In *Arabidopsis thaliana*, a positive relationship between temperatures from 19-28°C and
86 male meiotic recombination was previously described (Francis *et al.* 2007). However, this
87 temperature range represents only the upper portion of the viable range; *A. thaliana* can
88 flower and produce seeds also at much lower temperatures. Here we study the effect of
89 temperature on male meiotic recombination in *A. thaliana* across a wider temperature range
90 than it has been previously examined. We test whether lower and higher temperatures affect
91 class I and/or class II crossover frequency, and also explore whether changes in the length
92 of the chromosome axes and synaptonemal complex might suffice to explain the effects of
93 temperature on recombination rate in *A. thaliana*.

94

95

MATERIALS AND METHODS

96 **Plant growth**

97 Col-0 plants were grown under long day growth conditions (16h day 19-21°C / 8h night
98 15°C) until the primary inflorescence began to emerge from the rosette. Plants were then
99 transferred to a range of small, constant temperature, long-day growth chambers at the
100 experimental temperatures (5°C-30°C). For cytology, plants were grown to the same
101 developmental age and height after flowering and then transferred to growth chambers at
102 8°C, 18°C or 28°C for 1 week before material was collected to make slides. As the duration

103 of meiosis has previously been demonstrated to last 33 hours at 18.5°C (Armstrong *et al.*,
104 2003), 1 week was chosen to be long enough to complete meiosis at each temperature
105 without causing a significant impact on the developmental trajectory of the plants.
106 For flow cytometry, after transferring to constant temperature chambers, plants were
107 grown until at least 5-6 inflorescences had emerged and flowered, thus providing
108 sufficient pollen for flow cytometric analyses: 28°C, 23°C – 1 week, 18°C – 2 weeks, 13°C
109 – 3 weeks, 8°C – 5 weeks.

110

111 **Seed set**

112 Seed set was quantified as seeds per silique. For each temperature seeds were counted for 3-
113 10 siliques for each of 3-4 biological replicates (plants). All siliques originated from the
114 primary inflorescence.

115

116 **Pollen viability**

117 *Method 1:* For each temperature pollen viability was determined by Alexander staining for 2-
118 4 plants. For each plant ~200 pollen grains were counted. All flowers originated from the
119 primary inflorescence. Pollen viabilities reported are the means of the biological replicates
120 for each temperature. *Method 2:* When analyzing flow cytometry data, single pollen grains
121 were subdivided into two populations (viable and non-viable) based on SSC/FSC (Figure
122 S9A-C). To confirm their composition, the two populations were sorted using a MoFlo
123 ASTRIOS (Beckman-Coulter), stained using Alexander's stain (10%) and viewed under a
124 light microscope (Figure S9D-G). While the presumed non-viable population consisted solely
125 of non-viable pollen grains, the presumed viable population contained both viable and non-
126 viable pollen grains (Figure S9D-H). This method therefore provides an output proportional
127 to pollen viability, but systematically over-estimates pollen viability.

128

129 **Pollen fluorescence detection**

130 For each Fluorescent Tagged Line (FTL) and each temperature, flowers were collected for a
131 minimum of three pools of three plants, each pool representing one biological replicate.
132 Pollen was isolated and analysed as described in Yelina *et al.* (2013). An LSR Fortessa (BD)
133 was used for analysis, with 440nm, 488nm and 561nm lasers and 470/20, 530/30 and 582/15
134 bandpass filters used for detection of eCFP, eYFP and dsRED respectively. A standard run
135 consisted of 50,000-100,000 pollen grains for each biological replicate.

136

137 **Analysis of flow cytometry data**

138 Single viable pollen grains were first subset based on size and granularity parameters,
139 forward scatter (FSC) and side scatter (SSC) respectively (Figure S9A-C). Due to loss of
140 fluorescent signal (but not loss of the respective transgene) in a significant proportion of
141 pollen grains, a gating strategy was first used to eliminate potential false negatives prior to
142 recombination analysis. Using this strategy, pollen grains were first subset based on
143 detection of the “control” fluorophore and then scored for recombination based on the
144 presence/absence of the “diagnostic” fluorophore (Figure S10A-D). The fluorophore used as
145 the control had the less stable signal and the diagnostic fluorophore had the more stable
146 signal. This ensured that for pollen grains used in analysis, loss of signal was due to
147 recombination (i.e. true absence of the transgene) rather than a false negative loss of signal
148 (Figure S10E-F).

149 A similar approach using two diagnostic fluorophores was used to detect double crossovers
150 (DCOs, Figure S11). Although reciprocal results (e.g. eCFP⁺/eYFP^{+/-} vs eYFP⁺/eCFP^{+/-})
151 gave relatively consistent recombination frequencies (Figures S10-11), there were some
152 discrepancies. To assess which fluorophore detection regime gave the most accurate results
153 we exploited the fact that for intervals Ia and Ib: $SCO_{Ia} + SCO_{Ib} = SCO_{Iab} + 2*DCO_{Iab}$. For
154 each regime we assessed the concordance between $(SCO_{Ia} + SCO_{Ib})$ and $(SCO_{Iab} + 2*DCO_{Iab})$
155 and used the regime that gave the most concordant results in all further analyses (e.g. Figure
156 S12).

157

158 **Beam film modelling and analysis**

159 Best-fit parameters for the FTL intervals on chromosomes 3 and 5 were determined using
160 MADpatterns (White *et al.* 2017) and custom perl scripts, using an approach based on that
161 described in (Zhang *et al.* 2014). Parameter value ranges (Smax: 1 - 8.5; L: 0.7 - 1; T2 Prob:
162 0.0025 - 0.011; cL: 0.9 - 1.6 and cR: 0.9 - 1.6) were chosen based on parameter values
163 described in Zhang et al (2014) and comparison of ad hoc simulations with analysis of a large
164 Arabidopsis whole genome recombination dataset described in (Basu-Roy *et al.* 2013). Final
165 best-fit parameters for the FTL intervals were identified by comparing simulated data with
166 the experimental FTL data.

167 Crossovers were simulated using a range of parameter combinations (50,000 bivalents per
168 parameter set): parameters Smax, L, T2 Prob, cL and cR were varied, while parameters B,
169 Bmax, A and M were set at appropriate default values (Zhang *et al.* 2014). The number of
170 precursor sites (N) was calculated based on the total number of DSBs expected per meiosis in

171 Arabidopsis (~250) multiplied by the proportion of the genome length contributed by the
172 chromosome being simulated. Appropriate values for the position and strength of
173 recombination “black holes” (Bs, Be, Bd) – corresponding to recombination suppressed
174 centromeres – were chosen based on the analysis of experimental data in (Basu-Roy *et al.*
175 2013). Simulated chromosomes were analysed for crossover distribution and coefficient of
176 coincidence (CoC) in the regions of the simulated chromosomes corresponding to the
177 respective FTL intervals using the procedure outlined in (White *et al.* 2017). For each
178 parameter set, the simulated recombination frequencies and CoC values were compared to
179 values derived from the experimental FTL data. Importantly the experimental data are gamete
180 data, while the MADpatterns program simulates (and outputs) bivalent data (i.e. for a
181 chromosome pair). Therefore, all simulated bivalent crossover frequencies were halved to
182 convert to gamete crossover frequencies. Parameter sets were then ranked, first based on the
183 difference between the simulated and experimentally determined CoC values [$\text{Score}_{\text{CoC}} =$
184 $(\text{CoC}_{\text{sim}} - \text{CoC}_{\text{FTL}})^2$] and secondly based on the difference between the observed FTL
185 recombination frequencies and the simulated (gamete) recombination frequencies of the two
186 intervals [$\text{Score}_{\text{RF}} = \text{abs}\{\log_2(\text{RFI1}_{\text{sim}}/\text{RFI1}_{\text{FTL}})\} + \text{abs}\{\log_2(\text{RFI2}_{\text{sim}}/\text{RFI2}_{\text{FTL}})\}$]. The final
187 parameter values chosen (Table 1) were those with the lowest rank-sum. At least three rounds
188 of analysis, with progressively smaller step-sizes between values were used to arrive at the
189 final parameter values.

190 Finally, we modelled the effects on CoC, of increased crossovers caused by changes in a
191 single parameter of the MADpatterns program (either Smax, L or T2 prob). For each
192 parameter, the value was adjusted until a ~13% increase in COs had been achieved (i.e. the
193 average increase in COs observed between 18°C and temperature extremes; Table 1), the
194 changes in CoC predicted for each parameter change were then compared to those
195 observed experimentally (Figure 2).

196

197 **Cytological procedures**

198 Immunolocalisation slides using fresh material and DAPI stained spreads using acid fixed
199 material were prepared as described previously (Caryl *et al.* 2000; Armstrong *et al.* 2002).
200 The following antibodies and dilutions were used: anti-AtMLH1 (rat, 1/200 dilution)
201 (Higgins *et al.* 2005), anti-AtHEI10 (rat, 1/200 dilution, rabbit, 1/200 dilution) (Lambing *et al.*
202 *et al.* 2015), anti-AtZYP1 (rabbit, 1/500 dilution, guinea-pig, 1/500 dilution) (Higgins *et al.*
203 2005), FITC anti-guinea-pig (1/100, Abcam), alexa-fluor 488 anti-rat (1/500, ThermoFisher),
204 alexa-fluor 594 anti-rabbit (1/500, ThermoFisher), alexa-fluor 555 anti-rat (1/800, Abcam)

205 and alexa-fluor 647 anti-rabbit (1/800, Abcam). Epifluorescence microscopy was carried out
206 using a Nikon 90i Fluorescence Microscope (Tokyo, Japan) and image capture, analysis and
207 processing were conducted using NIS-Elements software (Nikon, Tokyo, Japan). Structured
208 illumination microscopy was carried out using a Zeiss Elyra PS1 and image reconstruction
209 and channel-alignment were carried out using ZEN black software (Zeiss). SC length
210 measurements were made by measuring total SC length in three dimensions using the simple
211 neurite tracer plugin to imageJ with Z-stacked images of pachytene nuclei stained for ZYP1
212 (Longair *et al.* 2011). Measurements were only taken from cells in which 5 complete
213 bivalents could be measured to ensure cells were fully synapsed and the 5 bivalent lengths
214 were combined to give a total SC length for each cell. MLH1 and HEI10 foci were identified
215 as bright, round foci that overlapped with the SC in the x, y and z planes and were observed
216 in late pachytene/early diplotene cells which were identified as either being fully synapsed or
217 mostly synapsed with some small regions of SC disassembly, respectively. Note, HEI10 and
218 MLH1 foci numbers in *Arabidopsis* have previously been shown to remain constant from late
219 pachytene through diplotene (Chelysheva *et al.* 2012). Mann-Whitney U-tests were used to
220 compare MLH1 and HEI10 foci counts and total SC lengths as described previously
221 (Ziolkowski *et al.* 2017). This was appropriate as bulked anthers from multiple plants
222 exposed to the same temperature treatment were used when making each immunolocalisation
223 slide and therefore each cell was treated as an independent observation.

224

225 **Data availability**

226 Data are available by request from the authors.

227

228

RESULTS

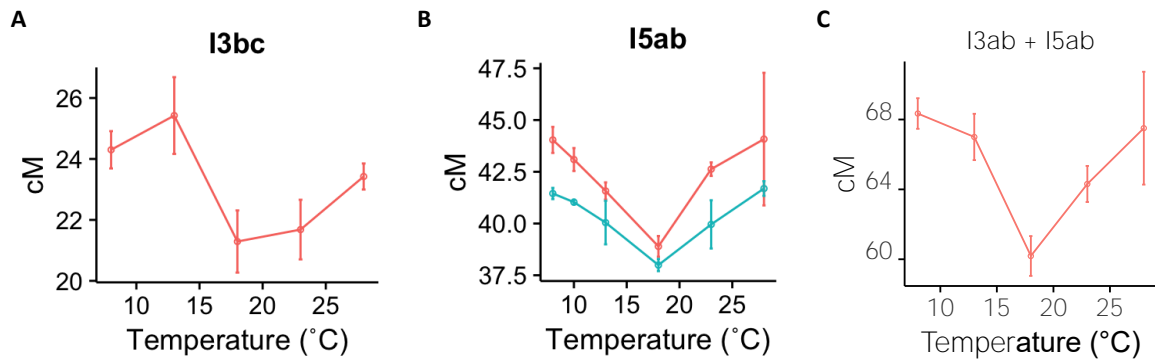
229 **Crossover rates in *Arabidopsis* are lowest in the middle of the fertile temperature** 230 **range**

231 We measured recombination both in meiocytes and in gametophytes. In the latter,
232 recombination rate estimates can be confounded because: (1) recombination declines
233 sharply due to structural failures when temperatures exceed failure thresholds, thus a biased
234 view can arise if temperatures past the failure points are included, and/or (2) estimates can
235 be biased due to failures in later stages of gametophyte development. Both sources of bias
236 can be averted at least to some extent by avoiding temperatures that cause a decline in
237 fertility. Thus, we first estimated the informative temperature range for *A. thaliana* by
238 measuring seed set and pollen viability at temperatures from 5°C to 30°C. At the high end,

239 seed set dropped significantly from 28°C to 30°C (Figure S1). At 8°C seed set was no
240 different from seed set at moderate temperatures (18°C, $p = 1$; 23°C, $p = 1$; t-test, Bonferroni
241 corrected), however there was no seed set at 5°C (Figure S1). The latter is consistent with
242 previously observed post-meiotic defects following 4-5°C cold-stress (De Storme *et al.*
243 2012). Therefore, for our purposes, we defined the “fertile range” of *A. thaliana* in our
244 conditions as 8°C to 28°C and focused on this range to assay recombination. Within this
245 temperature range there was no significant decrease in pollen viability at temperature
246 extremes, although variance increased at higher temperature (Figure S2). We also
247 ascertained that we had not exceeded failure thresholds using cytological observations. In
248 plants exposed to 8°C, 18°C or 28°C for 1 week synapsis, CO formation and chromosomal
249 segregation proceeded without appreciable errors in male meiocytes (Figure S3) and at
250 neither temperature extreme were obvious differences evident relative to 18°C.

251

252 To initially score recombination rates at different temperatures in high throughput, we
253 capitalized on a previously developed transgenic tool that uses fluorescent markers to score
254 male meiotic crossovers in pollen grains (Francis *et al.* 2007). We scored male crossover
255 frequency in Fluorescent Tagged Lines (FTLs) that flank two pairs of adjacent intervals on
256 chromosome 3 (I3b and I3c) and chromosome 5 (I5a and I5b). While the FTL loci showed
257 subtle differences in the responses at different temperatures (Figure 1 & S4-S5), the overall
258 shapes of the I3bc and I5ab distributions were not significantly different after normalizing
259 for the different sizes of the intervals ($p = 0.873$, Two-sample Kolmogorov-Smirnov test).
260 Both pairs of intervals followed the same general trend with a minimum recombination rate
261 at ~18°C and higher frequencies at both higher and lower temperatures (Figure S4-S5). The
262 combined genetic length of the four intervals shows a clear U-shaped trend of recombination
263 rates across the temperature range (Figure 1C). Using a Mann-Whitney-Wilcoxon Rank Test
264 (unpaired Wilcoxon test) on combined data from the four intervals, we found crossover rates
265 were significantly lower (10-15 %) at 18°C, the center



266

267

268

269

270

271

272

273

274

275

276

277

278

279

280

281

282

283

284

285

286

287

288

289

290

291

292

Figure 1. Meiotic recombination has a U-shaped response to temperature in Arabidopsis. Data from intervals I3bc and I5ab demonstrate a U-shaped response in recombination rate to temperature (A & B). For interval I5ab (B), the same trend is observed when plants have different numbers of secondary bolts and branches across the temperature range (red) or if all plants are harvested when they have 5-6 inflorescences (blue). The combined genetic length of intervals I3bc and I5ab is shown in (C). Error bars indicate 95% confidence intervals.

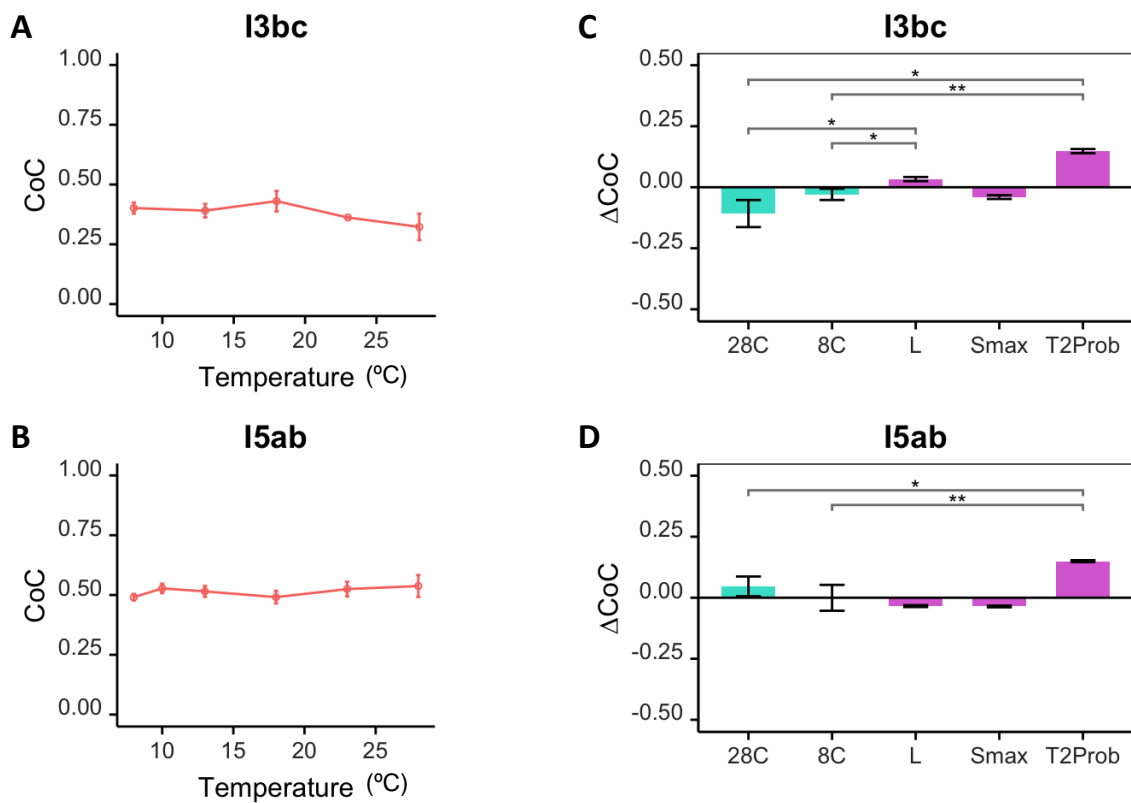
of the fertile temperature range, than at either 8°C or 28°C ($p = 7.76e^{-6}$ and $p = 2.22e^{-5}$ respectively). The upper half of the trend recapitulates previous findings in *A. thaliana* (assayed with markers on a different chromosome) of a positive trend from 19-28°C (Francis *et al.* 2007). Since recombination rates can also be sensitive to developmental age (Francis *et al.* 2007) we tested whether this trend was merely a consequence of differences in overall development at the different temperatures (Figures 1B & S6). By assaying only plants at comparable developmental stages i.e. all plants with 5-6 inflorescences (Figure S6B), we showed that the increase in recombination rate at lower as well as higher temperatures is still evident. This indicates that *A. thaliana*, like *Drosophila* and several other species (Bomblies *et al.* 2015), has a U-shaped relationship between temperature and recombination rate.

Modeling predicts increased crossovers occur via the class I pathway

We next explored which crossover pathways might be affected. In *A. thaliana*, the majority (85%) of crossovers are class I crossovers; these rely absolutely on a group of proteins called the ZMM proteins and are subject to crossover interference, which prevents crossovers occurring in close proximity (Mercier *et al.* 2005; Chelysheva *et al.* 2007; Higgins *et al.* 2008; Chelysheva *et al.* 2012; 37–39). The remaining crossovers are collectively referred to

293 as class II crossovers; these occur via several pathways, and are not sensitive to crossover
 294 interference (Berchowitz et al. 2007; Higgins et al. 2008). When measured genetically (as
 295 here) the Coefficient of Coincidence (CoC) - the number of double crossovers observed,
 296 divided by the number expected in a given pair of intervals based on the single crossover
 297 rates - can provide insight into the relative contributions of the class I and class II crossover
 298 pathways (CoC should increase if additional crossovers are primarily class II non-interfering
 299 crossovers). For both pairs of intervals (I3b/I3c and I5a/I5b), we calculated CoC across the
 300 temperature range and observed no change, or a slight decrease in CoC at temperature
 301 extremes. This observation indicates that crossovers do not become noticeably more likely
 302 to occur near one another at higher or lower temperatures, suggesting that the increase in
 303 recombination rates may primarily involve class I (interfering) rather than class II crossovers
 304 (Figure 2A-B).

305



306

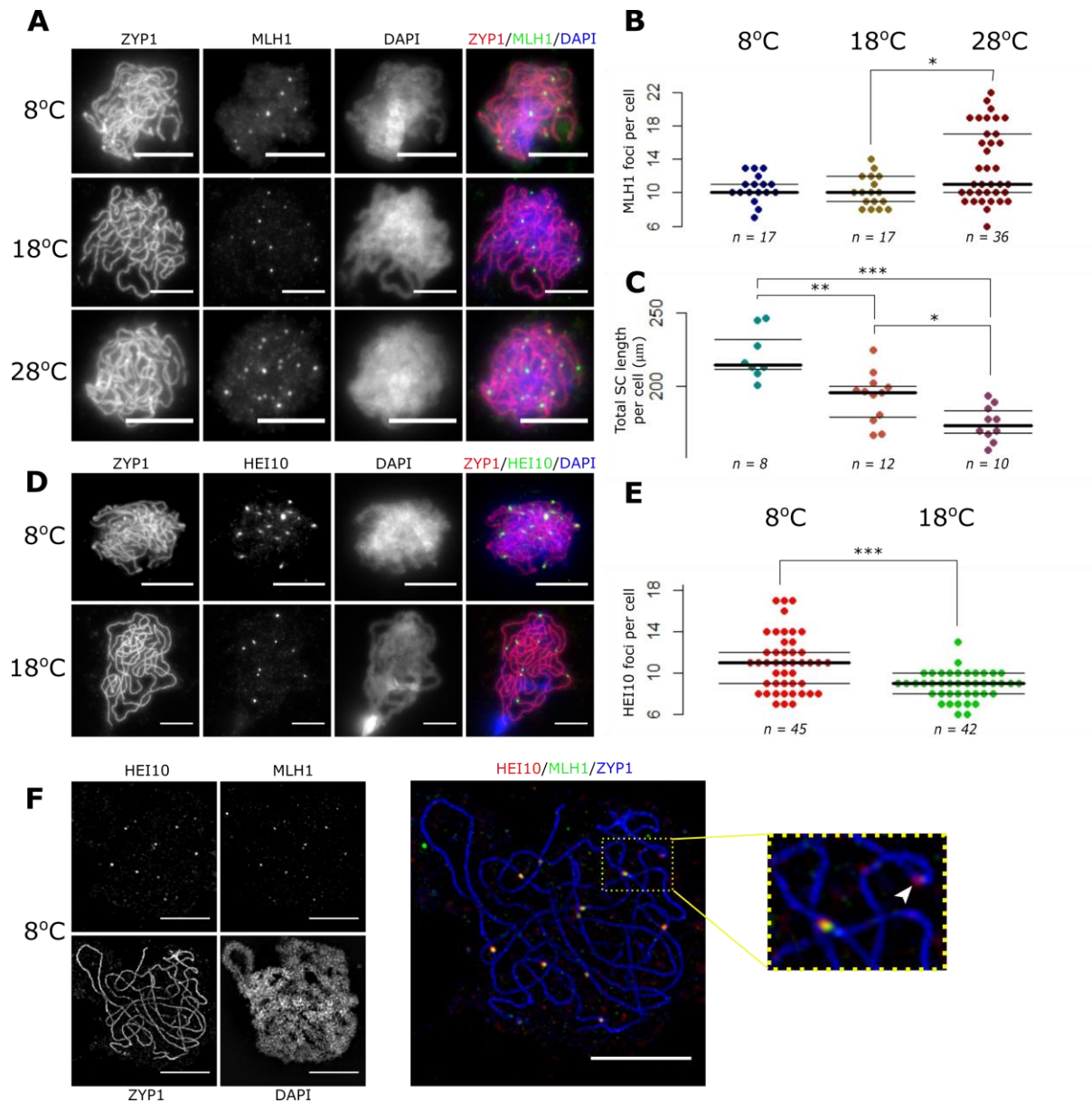
307 **Figure 2. Observed and predicted CoC for intervals I3bc and I5ab.** For I3bc (A) and I5ab
 308 (B), CoC values were mostly constant across the temperature range, although for I3bc CoC
 309 was slightly lower at 28°C than at 18°C ($p = 0.018$; pairwise t-test with Bonferroni
 310 correction). (C & D) The change in CoC observed between 18°C and 28°C or 8°C is shown
 311 in teal; the change in CoC predicted by changes in a single beam film model parameter that

312 results in a 13% increase in COs (i.e. the average increase observed at temperature extremes)
313 is shown in purple. Observed changes in CoC are consistent with changes predicted by
314 altering beam film model parameters that affect class I COs – L, the proportion of the
315 chromosome over which interference spreads and/or Smax, the (class I) crossover
316 designation driving force. The observed changes in CoC are not consistent with changes
317 predicted by altering the number of class II COs (T2Prob). Error bars indicate 95%
318 confidence intervals.

319

320 We further tested this idea by simulating crossover patterning under the beam film model, a
321 leading model of crossover designation and interference (White *et al.* 2017). The beam-film
322 model proposes a mechanical basis of CO designation. Under this model, redistribution of
323 mechanical stress along the chromosomes is the basis of CO interference. COs occur at
324 precursor sites (i.e. meiotic DSBs) in regions of high stress, and locally relieve stress,
325 preventing the formation additional COs nearby. Three important parameters of the beam
326 film model are: “Smax” - the crossover designation driving force, “L” – the proportion of
327 the chromosome over which interference propagates (i.e. proportion of the chromosome
328 over which stress is relieved), and “T2prob” – the proportion of potential crossover sites
329 that develop into non-interfering Class II crossovers. Changes in these parameters affect the
330 crossover frequency and CoC predicted by the model. We determined the best-fit parameters
331 for the intervals I5ab and I3bc in male meiosis (Table 1) using the experimental FTL data
332 and a previously published large recombination dataset (Basu-Roy *et al.* 2013). We then
333 adjusted single parameter values (Table 1) to model an increase in crossovers equivalent to
334 that observed at higher and lower temperatures. We compared the observed CoC to the
335 changes predicted by the beam film model under different parameter values. When extra
336 crossovers were simulated to occur via the class I (interfering) pathway, the predicted effects
337 on CoC were consistent with our observations (Figure 2C – Smax; Figure 2D – Smax, L),
338 but when extra crossovers were simulated to occur via the class II (non-interfering) pathway,
339 the predicted changes in CoC were not consistent with observed changes (Figure 2C-D).
340 Consistent with the hints from the CoC trends, the modelling suggests increased crossovers
341 observed as temperature changes in *A. thaliana* occur exclusively or primarily via the
342 interference sensitive class I (ZMM) pathway.

343



344

345 **Figure 3. An increase in total class I CO frequency is observed at high and low**
 346 **temperature extremes and increasing temperature is associated with shorter SC**
 347 **length.** MLH1 foci were counted in pachytene cells stained for ZYP1, MLH1 and DAPI
 348 (A) from plants grown for 1 week at 8, 18 and 28 °C. A plot showing MLH1 foci counts
 349 (B) demonstrates a significant increase in total class I CO number at 28 °C compared to 18
 350 °C. Total SC lengths per cell in μm (C) also decrease significantly with increasing
 351 temperatures. HEI10 foci were also counted in pachytene cells stained for ZYP1, HEI10
 352 and DAPI (D) from plants grown for 1 week at 8 or 18 °C. A plot showing HEI10 foci
 353 counts (E) demonstrates a significant increase in total class I CO number at 8 °C compared
 354 to 18 °C. A cell stained for HEI10, MLH1, ZYP1 and DAPI and imaged using structured-
 355 illumination microscopy (F) confirms that additional HEI10 foci are present that are not

356 associated with corresponding MLH1 foci (indicated by arrowhead) in plants grown for 5
357 weeks at 8 °C. Scale bars = 5 μm. * $p < 0.05$, ** $p < 0.005$, *** $p < 0.0005$.

358

359 **Increased crossovers occur via the class I pathway**

360 To empirically test whether the class I / ZMM dependent crossovers are indeed responsible
361 for the observed increases in recombination at high or low temperature, we quantified the
362 number of MLH1 foci. MLH1 is a member of the MutL complex together with MLH3 and
363 marks sites of class I crossovers (White *et al.* 2017). We counted MLH1 foci in pachytene
364 nuclei from plants exposed to 8°C, 18°C or 28°C for 1 week (Figure 3A). We found a
365 significant increase in MLH1 foci when comparing 18°C and 28°C (Mann-Whitney U Test,
366 $p = 0.01681$) indicating that high temperature does cause an increase in Class I crossovers
367 as predicted by the modeling. However, we did not observe an increase in MLH1 foci at 8°C
368 (1 week or 6 weeks) compared to 18°C (Mann-Whitney U Test, $p = 0.4299$ & $p = 0.503$
369 respectively; Figure 3B & S7).

370

371 While the low temperature results are at first pass puzzling in the context of modeling
372 predictions, there is some evidence that MLH1 independent class I crossovers can occur in
373 Arabidopsis: loss of any of several ZMM proteins (and hence all class I crossovers) result
374 in an 85% reduction in crossovers (e.g., Stern 1926; Wilson 1959) while loss of MLH3, and
375 therefore functional MutL complex (MLH1/MLH3), results in only a 60% reduction
376 (Jackson *et al.* 2006). Thus, we reasoned that low temperature might increase recombination
377 rate via such MLH1-independent class I crossovers. We therefore quantified foci of another
378 class I crossover associated protein, HEI10 (Figure 3D) at both 8°C and 18°C. In contrast to
379 MLH1, which is observed from pachytene and only marks sites of future crossovers (White
380 *et al.* 2017), HEI10 foci are observed early in meiotic prophase I and initially mark many
381 precursor sites not destined to become crossovers (Chelysheva *et al.* 2012). The number of
382 HEI10 foci then reduces until only sites destined to become crossovers are marked by
383 pachytene (Chelysheva *et al.* 2012). For this reason, we only counted HEI10 foci in late
384 pachytene cells in which all five pairs of chromosomes were completely synapsed or in early
385 diplotene cells in which the synaptonemal complex is just beginning to dissociate. We found
386 a significant increase in HEI10 foci at 8°C relative to 18°C (Mann-Whitney U Test, $p =$
387 0.0001316). We also observed a significant increase in HEI10 foci compared to MLH1 foci
388 at 8°C (Mann-Whitney U Test, $p = 0.01543$) although no difference between HEI10 or
389 MLH1 foci was observed at 18°C (Mann-Whitney U Test, $p = 0.7198$). In agreement with a

390 higher number of HEI10 foci at 8°C, most cells at 8°C had 1-2 HEI10 foci that did not co-
391 localize with MLH1 (Figure 3F). Taken together, these results suggest that in *A. thaliana*
392 the increased crossover frequency at both high and low temperatures involves an increase
393 in class I interfering crossovers, though the low and high temperature effects are
394 mechanistically at least somewhat distinct.

395

396 **The class II pathway does not contribute to increased crossovers**

397 Though our modeling suggested that Class II crossovers are not likely to be involved in the
398 temperature trends we observed in *A. thaliana*, in yeast, class II crossovers had been
399 previously reported to increase in number with low temperatures in some mutant contexts
400 (Mercier *et al.* 2014). Thus we also wished to test whether class II crossovers might
401 contribute to the temperature effect on recombination in our study. Since there is no robust
402 cytological marker for non-interfering crossovers in *A. thaliana*, we used recombination
403 assays in mutant lines that lack class I crossovers. First, we repeated the pollen based
404 recombination assay for FTL line I3bc in a *zip4, fancm* double mutant. In *A. thaliana*, *zip4*
405 mutants lack class I crossovers, leading to semi-sterility (Chelysheva *et al.* 2007) while
406 *fancm* mutants have increased class II crossovers (Crismani *et al.* 2012). This increase in
407 crossovers restores pollen viability to the double *zip4, fancm* mutant under standard growing
408 conditions (Crismani *et al.* 2012), enabling the pollen based FTL assay to be used. In the
409 *fancm, zip4* background, crossover levels were unchanged at 28°C compared to 18°C (Figure
410 S8A; $p = 0.986$, pairwise t-test with Bonferroni correction), confirming that increased
411 recombination at high temperature occurs exclusively or primarily via the class I pathway.
412 Crossover number increased at low temperature with borderline significance (10°C vs 18°C,
413 $p = 0.058$, pairwise t-test with Bonferroni correction, Figure S8A). However, pollen viability
414 was also drastically reduced in these double mutants at temperatures below 18°C, suggesting
415 that FANCM becomes more important at lower temperatures, at least in the absence of class
416 I crossovers (Figures S8B & S9).

417

418 While the results for *zip4, fancm* double mutants at low temperature might suggest an
419 increase in Class II crossovers at low temperatures in *A. thaliana*, similar to that observed
420 at low temperature in yeast *zmm* mutants, we were concerned that (1) low pollen viability
421 may have introduced a sampling bias in the double mutant at low temperature or (2) the
422 unanticipated requirement for FANCM at lower temperatures in the absence of Class I
423 crossovers may have affected our results in complex ways that are not necessarily relevant

424 in a wild type context. We therefore used a second cytological assay to investigate the effect
425 of low temperature on class II crossovers, performing chiasma counts on metaphase I cells
426 from *msh5* mutants after exposure to either 8°C or 18°C for 1 week. MSH5, a ZMM protein,
427 is absolutely required for class I crossovers, and the only chiasmata that remain in an *msh5*
428 mutant occur via the class II pathway (Higgins *et al.* 2008). Unlike FANCM, MSH5 does
429 not affect the class II pathway. We found that in this mutant there was no significant
430 difference in chiasma counts between 8°C (n = 56 cells, mean chiasma number = 1.44) and
431 18°C (n = 85 cells, mean chiasma number = 1.46; χ^2 Test, $p = 0.792$; Figure S7). Unlike the
432 pollen-based recombination assay we used for the *zip4*, *fancm* double mutants, the
433 metaphase I bivalent counts occur before any potential sampling bias is introduced due to
434 low pollen viability, and therefore likely better represents the effect of temperature on class
435 II crossovers. These results suggest that the number of class II crossovers remains essentially
436 unchanged across the tested temperature range in *A. thaliana*.

437

438 **Synaptonemal complex length is negatively correlated with temperature**

439 A previous study in barley demonstrated that a slightly increased crossover frequency at
440 higher temperatures was associated with a concurrent increase in chromosome length as
441 measured by the length of the synaptonemal complex (SC), suggesting that the longer
442 chromosome length might explain the increase in crossover rate at higher temperatures
443 (Phillips *et al.* 2015). SC length is also known to positively correlate with CO numbers in
444 mammals (Lynn *et al.* 2002). We therefore measured total SC length in our MLH1/ZYP1
445 stained pachytene cells from *A. thaliana* grown at different temperatures to ask whether the
446 same trend is seen (Figure 3C) (ZYP1 is the synaptonemal central element protein of *A.*
447 *thaliana*, (Higgins *et al.* 2005). In contrast to barley, we observed that in *A. thaliana* total
448 SC length significantly *decreased* with increasing temperatures and that this was consistent
449 (a linear decline) across the whole temperature range (Mann-Whitney U Test, 8°C vs 18°C
450 $p = 0.001064$, 18°C vs 28°C $p = 0.0169$, 8°C vs 28°C $p = 0.0000457$). Thus in *A. thaliana*
451 the increase in crossover number at elevated temperatures cannot be explained by an
452 increase in SC length. However, the low temperature effect could be: When factoring in the
453 observed 14% ($28 \pm 8 \mu\text{m}$) increase in SC length at 8°C relative to 18°C, the beam film
454 model predicts a 16% increase in class I crossovers (or a 14% increase in total
455 recombination). This is consistent with the observed increases in recombination measured
456 by the pollen-based assay (8–18% increase in total recombination) and HEI10 foci counts
457 (14–34% increase in class I crossovers).

458

459

DISCUSSION

460

461

462

463

464

465

466

467

468

469

470

471

472

473

474

475

476

477

478

479

480

481

482

483

484

485

486

487

488

489

490

491

In this study, we demonstrate that male meiotic recombination rate increases at temperatures both above and below a nadir at 18°C in the Col-0 strain of *A. thaliana*. We show that both the high and low temperature increase appear to result wholly or mostly from an increase in class I interfering crossovers, but that the high temperature and low temperature effects may be mechanistically at least somewhat distinct. The low temperature increase in HEI10-marked, but MLH1-negative foci may be explainable by a concomitant increase in axis length of about 14% at lower temperatures. At high temperatures, on the other hand, axis length decreases, and thus cannot explain an increase in MLH1 foci and recombination.

There are reasons to think the effect of temperature on recombination may be in large part biophysical. For example, the length and integrity of the synaptonemal complex, which is which correlates with recombination rates (Zickler and Kleckner 2015), is known to be affected by temperature (e.g. Phillips *et al.* 2015; Rog *et al.* 2017). The recent observation that the synaptonemal complex displays liquid crystal like properties (Rog *et al.* 2017) suggest one possible mechanism. Liquid crystal structures could be easily perturbed by temperature, and indeed, extreme temperatures can lead to aberrant synaptonemal complex polymerization into polycomplexes (see Morgan *et al.* 2013). But this could also have important implications in understanding how recombination responds to subtler temperature changes, since even minor perturbation in the synaptonemal complex can cause quantitative effects on recombination frequency (Higgins *et al.* 2005). Liquid crystal properties of the SC could also provide a possible explanation for our observation that low temperature may increase the frequency of a specific sub-set of MLH1-independent, but ZMM dependent (class I) crossovers. If the SC is less fluid at lower temperature it may be able to stabilize Holliday junctions without an absolute requirement for the MutL complex.

A variety of stresses other than temperature also affect recombination rates (De Storme and Geelen 2014; Bomblies *et al.* 2015). If we envision the perturbations in meiosis as direct effects of temperature on the relevant proteins, how can these other effects be explained? Stress from a wide range of sources affects the oxidative state of the cell, which can also affect protein function and stability directly. Interestingly, one protein that is known to be very responsive to oxidative state is the cohesin subunit REC8 (Perkins *et al.* 2016), which is important for axis emplacement and recombination (Molnar *et al.* 1995; Bai *et al.* 1999;

492 Cai *et al.* 2003). Cohesin failures can, in turn, mimic temperature-related failures,
493 specifically in the aggregation of axis proteins. These similarities suggest cohesin may be a
494 particularly sensitive component of meiosis and that its perturbation can have reverberating
495 effects through the subsequent processes of axis formation and recombination. Other factors
496 may also play a role. It is known, for instance, that abscisic acid signaling and chromatin
497 decondensation increase in response to temperature stress (Pecinka *et al.* 2010; Finkelstein
498 2013), and both are associated with increased recombination (Yin *et al.* 2009; Henderson
499 2012).

500

501 Our data suggest that temperature affects exclusively or primarily class I interfering
502 crossovers in *A. thaliana*. This is in line with reports in barley that Class I crossovers are
503 repositioned under warmer temperatures (Phillips *et al.* 2015). The barley study did not
504 examine class II crossovers, but in yeast, class II crossovers have been reported to increase
505 under temperature stress (Börner *et al.* 2004). This contrasts our findings in *A. thaliana*,
506 where Class II crossovers showed no response to temperature, suggesting there may be
507 variation among taxa in the sensitivity of particular crossover pathways to temperature. Such
508 variation could result if specific proteins involved in different aspects of meiosis have
509 different thermosensitivities across taxa. In mice and lilies, for example, there is evidence
510 that particular recombinases are directly sensitive to temperature (Hotta *et al.* 1985; Stern
511 1986; Hotta *et al.* 1988), which may play a role here too. Another possible explanation may
512 be a shift in crossover maturation dynamics. Previous experiments in yeast demonstrated
513 that low temperatures can affect the dynamics of early steps in meiotic recombination
514 (Börner *et al.* 2004), which may cause some crossovers to mature earlier or later at low
515 temperature, and could affect crossover rates as well as the presence of (or our ability to
516 detect) MLH1 foci at late pachytene. In barley, a change in the dynamics of DNA
517 replication, specifically the replication of heterochromatic DNA, can affect the ultimate
518 positioning of crossover events, though in this species it has negligible effects on their
519 number (Higgins *et al.* 2012). Together with results from yeast, this hints that the timing of
520 different stages of early meiotic events can alter crossover outcomes, though the details of
521 how temperature affects the timing of meiotic events in *A. thaliana* has yet to be described
522 in detail. Another factor may be that the SC is longer at lower temperatures, which could
523 provide more physical space for crossovers to form (e.g. Lynn *et al.* 2002; Phillips *et al.*
524 2015).

525

526 Our results are consistent with the idea that meiotic recombination is tuned to the
527 environment of a given species (Bomblies *et al.* 2015; Wright *et al.* 2015). The change in
528 recombination that occurs under temperature increases or decreases in most species is a
529 plastic response that is either adaptive in itself (Ritz *et al.* 2017) and/or reflects unavoidable
530 instability in the system (Morgan *et al.* 2017). Plasticity of recombination has been
531 previously described as a possibly adaptive response in some circumstances to increase
532 diversity in offspring (Modlizewski and Copenhaver 2015). However, considering how
533 common it is, we favor the idea that recombination rate plasticity, rather than being a directly
534 selected trait, is an unavoidable by-product of the thermosensitivity of core meiotic proteins
535 and/or processes, and that any benefits that arise from the increase in recombination are
536 inadvertent (Morgan *et al.* 2017). Nevertheless, even if it is just a happy accident, it may
537 well be that increasing recombination under temperature deviations does in fact benefit
538 future generations by facilitating rapid adaptation.

539

540 U-shaped curves in response to temperature suggest that in “optimal” conditions, organisms
541 generally have lower recombination rates than under stressful conditions. This is somewhat
542 surprising given that elevated recombination rates may be advantageous for adaptation in at
543 least some circumstances (e.g. Barton 1995; Charlesworth and Barton 1996; Presgraves
544 2005; Otto 2009; Campos *et al.* 2015). Indeed, numerous empirical studies have shown that
545 strong artificial selection for a wide variety of traits is correlated with an increase in
546 recombination rates (e.g. Flexon *et al.* 1982; Korol and Iliadi 1994; Ross-Ibarra 2004).
547 However, a potential explanation for why there might be a low-point in recombination is
548 that in a stable environment to which an organism is well adapted, minimizing
549 recombination (while still ensuring at least one crossover per bivalent) better maintains
550 allelic combinations that have been selected in previous generations (Otto 2009). An
551 additional possibility is that recombination, while important for chromosome segregation in
552 most species, is also mutagenic, and thus may be selected against (Arbeithuber *et al.* 2015).
553 Moreover, there is an important exception to the aforementioned trend that selection tends
554 to increase recombination. For example, when selection is applied for high fertility in mice,
555 recombination rates decline, suggesting that high recombination can decrease fertility and
556 may thus be evolutionarily selected against (Gorlov *et al.* 1992), even if no obvious
557 immediate defects are observed with even very high recombination rates (Girard *et al.*
558 2014).

559

560 There is evidence from several species that recombination rate may be linked with local
561 adaptation. For example, in grasshoppers, individuals with lower crossover rates are more
562 sensitive to temperature shock (Rees and Thompson 1958; Shaw 1971), while wild *Sordaria*
563 growing in distinct habitats have different recombination rates when grown together in
564 laboratory conditions (Saleem *et al.* 2001). There is also evidence that natural selection has
565 acted in populations adapted to different habitats on core meiotic proteins that have the
566 potential to affect recombination rates (Turner *et al.* 2008; Anderson *et al.* 2009; Wright *et*
567 *al.* 2015). The notion that temperature affects recombination and that populations adapt to
568 local prevailing climates, has important implications for interpreting observations of
569 recombination rate variation among populations when these are measured at a single
570 temperature in the lab. It may be, in at least some cases, that as populations adapt to distinct
571 environments, the recombination response curves shift in concert. If this is the case, when
572 measuring recombination rate at a single laboratory temperature, we may be sampling
573 different points on a given genotype's response curve, and may not be reflective of what
574 occurs in nature. For these reasons, it will be important to better understand both the causes
575 and the consequences of the links between stress, temperature, and meiotic recombination
576 (Bomblies *et al.* 2015) both from a mechanistic and evolutionary perspective.

577

578

ACKNOWLEDGEMENTS

579 We would like to thank Dr Eric Jenczewski for discussion of the manuscript. We thank Dr
580 Mathilde Grelon and Dr Ian Henderson for provision of the seeds for the FTL lines and Dr
581 Gregory Copenhaver who developed these lines. This work was supported by a European
582 Research Council Consolidator Grant to KB (CoG EVO-MEIO 681946), a Marie Curie
583 fellowship to AL (PIOF-GA-2013- 628128), and a BBSRC studentship to CM (DTP
584 BB/MO1116 x/1 M1BTP). This work has also been supported by the UK Biological and
585 Biotechnology Research Council (BBSRC) via grant BB/P013511/1 to the John Innes Centre.

586

587

REFERENCES

588

589 Anderson, J. A., W. D. Gilliland, and C. H. Langley, 2009 Molecular population genetics and
590 evolution of *Drosophila* meiosis genes. *Genetics* 181: 177–185.

591

592 Arbeithuber, B., A. J. Betancourt, T. Ebner, and I. Tiemann-Boege, 2015 Crossovers are
593 associated with mutation and biased gene conversion at recombination hotspots. *Proc. Natl.*
594 *Acad. Sci. U. S. A.* 112: 2109–2114.

595

596 Armstrong, S. J., A. P. Caryl, G. H. Jones, and F. C. H. Franklin, 2002 Asy1, a protein
597 required for meiotic chromosome synapsis, localizes to axis-associated chromatin in
598 *Arabidopsis* and *Brassica*. *J. Cell Sci.* 115: 3645–3655.
599

600 Armstrong, S. J., F. C. H. Franklin, and G. H. Jones, 2003 A meiotic timecourse for
601 *Arabidopsis thaliana*. *Sex. Plant Repr.* 16: 141–149.
602

603 Bai, X., B. N. Peirson, F. Dong, C. Xue, and C. A. Makaroff, 1999 Isolation and
604 characterization of SYN1, a RAD21-like gene essential for meiosis in *Arabidopsis*. *Plant Cell*
605 11: 417–30.
606

607 Barton, N. H., 1995 A general model for the evolution of recombination. *Genet Res.* 65: 123–
608 144.
609

610 Basu-roy, S., F. Gauthier, L. Giraut, and C. Mézard, 2013 Hot Regions of noninterfering
611 crossovers coexist with a nonuniformly interfering pathway in *Arabidopsis thaliana*. *Genetics*
612 195: 769–779.
613

614 Berchowitz, L. E., and G. P. Copenhaver, 2010 Genetic interference: don't stand so close to
615 me. *Curr. Genomics* 11: 91–102.
616

617 Berchowitz, L. E., K. E. Francis, A. L. Bey, and G. P. Copenhaver, 2007 The role of
618 AtMUS81 in interference-insensitive crossovers in *A. thaliana*. *PLoS Genet.* 3: 1355–1364.
619

620 Bilgir, C., C. R. Dombeki, P. F. Chen, A. M. Villeneuve, and K. Nabeshima, 2013
621 Assembly of the synaptonemal complex is a highly temperature-sensitive process that is
622 supported by PGL-1 during *Caenorhabditis elegans* meiosis. *G3* 3: 585–595.
623

624 Bomblies, K., J. D. Higgins, and L. Yant, 2015 Meiosis evolves: Adaptation to external and
625 internal environments. *New Phytol.* 208: 306–323.
626

627 Börner, G. V., N. Kleckner, and N. Hunter, 2004 Crossover / noncrossover differentiation,
628 synaptonemal complex formation, and regulatory surveillance at the leptotene /zygotene
629 transition of meiosis. *Cell* 117: 29–45.
630

631 Cai, X., F. Dong, R. E. Edelmann, and C. Makaroff, 2003 The *Arabidopsis* SYN1 cohesin
632 protein is required for sister chromatid arm cohesion and homologous chromosome pairing. *J.*
633 *Cell Sci.* 116: 2999–3007.
634

635 Campos, L., D. L. Halligan, P. R. Haddrill, and B. Charlesworth, 2015 The Relation between
636 recombination rate and patterns of molecular evolution and variation in *Drosophila*
637 *melanogaster*. *Mol. Biol. Evol.* 31: 1010–1028.
638

639 Caryl, A. P., S. J. Armstrong, G. H. Jones, and F. C. H. Franklin, 2000 A homologue of the
640 yeast HOP1 gene is inactivated in the *Arabidopsis* meiotic mutant *asy1*. *Chromosoma* 109:
641 62–71.
642

643 Charlesworth, B., and N. H. Barton, 1996 Recombination load associated with selection for
644 increased recombination. *Genet Res.* 67: 27–41.
645

646 Chelysheva, L., G. Gendrot, D. Vezon, M.-P. Doutriaux, R. Mercier, *et al.*, 2007 Zip4/Spo22
647 is required for class I CO formation but not for synapsis completion in *Arabidopsis thaliana*.
648 PLoS Genet. 3: e83.
649
650 Chelysheva, L., D. Vezon, A. Chambon, G. Gendrot, L. Pereira, *et al.*, 2012 The *Arabidopsis*
651 HEI10 is a new ZMM protein related to Zip3. PLoS Genet. 8: e1002799.
652
653 Crismani, W., C. Girard, N. Froger, M. Padrillo, J. L. Santos, *et al.*, 2012 FANCM limits
654 meiotic crossovers. Science 336: 1588–1590.
655
656 De Storme, N., G. P. Copenhaver, and D. Geelen, 2012 Production of diploid male gametes
657 in *Arabidopsis* by cold-induced destabilization of post-meiotic radial microtubule arrays.
658 Plant Physiol. 160: 1808–1826.
659
660 De Storme, N., and D. Geelen, 2014 The impact of environmental stress on male
661 reproductive development in plants: biological processes and molecular mechanisms. Plant
662 Cell Environ. 37: 1–18.
663
664 Elliott, C. G., 1955 The effect of temperature on chiasma frequency. Heredity 9: 385–398.
665
666 Finkelstein, R., 2013 Abscisic Acid synthesis and response. Arabidopsis Book 11: e0166.
667
668 Flexon, P. B., and C. F. Rodell, 1982 Genetic recombination and directional selection for
669 DDT resistance in *Drosophila melanogaster*. Nature 298: 672–674.
670
671 Francis, K. E., S. Y. Lam, B. D. Harrison, A. L. Bey, L. E. Berchowitz, *et al.*, 2007 Pollen
672 tetrad-based visual assay for meiotic recombination in *Arabidopsis*. Proc. Natl. Acad. Sci. U.
673 S. A. 104: 3913–3918.
674
675 Girard, C., W. Crismani, N. Froger, J. Mazel, A. Lemhemdi, *et al.*, 2014 FANCM-associated
676 proteins MHF1 and MHF2, but not the other Fanconi anemia factors, limit meiotic
677 crossovers. Nucleic Acids Res. 42: 9087–9095.
678
679 Gorlov, I., L. Schuler, L. Bunger, and P. Borodin, 1992 Chiasma frequency in strains of mice
680 selected for litter size and for high body weight. Theor. Appl. Genet. 84: 640–642.
681
682 Henderson, I. R., 2012 Control of meiotic recombination frequency in plant genomes. Curr.
683 Opin. Plant Biol. 15: 556–561.
684
685 Higgins, J. D., E. F. Buckling, F. C. H. Franklin, and G. H. Jones, 2008 Expression and
686 functional analysis of AtMUS81 in *Arabidopsis* meiosis reveals a role in the second pathway
687 of crossing-over. Plant J. 54: 152–162.
688
689 Higgins, J. D., R. M. Perry, A. Barakate, L. Ramsey, R. Waugh, *et al.*, 2012 Spatiotemporal
690 asymmetry of the meiotic program underlies the predominantly distal distribution of meiotic
691 crossovers in barley. Plant Cell 24: 4096–4109.
692
693 Higgins, J. D., E. Sanchez-Moran, S. J. Armstrong, G. H. Jones, and F. C. H. Franklin, 2005
694 The *Arabidopsis* synaptonemal complex protein ZYP1 is required for chromosome synapsis
695 and normal fidelity of crossing over. Genes Dev. 19: 2488–500.

696
697 Higgins, J. D., J. Vignard, R. Mercier, A. G. Pugh, and G. H. Jones, 2008 AtMSH5 partners
698 AtMSH4 in the class I meiotic crossover pathway in *Arabidopsis thaliana*, but is not required
699 for synapsis. *Plant J.* 55: 28–39.
700
701 Hotta, Y., M. Fujisawa, S. Tabata, H. Stern, and S. Yoshida, 1988 The effect of temperature
702 on recombination activity in testes of rodents. *Exp. Cell Res.* 178: 163–168.
703
704 Hotta, Y., S. Tabata, R. A. Bouchard, R. Piñon, and H. Stern, 1985 General recombination
705 mechanisms in extracts of meiotic cells. *Chromosoma* 93: 140–151.
706
707 Jackson, N., E. Sanchez-Moran, E. Buckling, S. J. Armstrong, G. H. Jones, *et al.*, 2006
708 Reduced meiotic crossovers and delayed prophase I progression in AtMLH3-deficient
709 *Arabidopsis*. *Embo J.* 25: 1315–1323.
710
711 Jensen, J., 1981 Effect of temperature on genetic recombination in barley. *Hereditas* 94: 215–
712 218.
713
714 Korol, A. B., and K. G. Iliadi, 1994 Increased recombination frequencies resulting from
715 directional selection for geotaxis in *Drosophila*. *Heredity* 72: 64–68.
716
717 Lambing, C., K. Osman, K. Nuntasontorn, A. West, J. D. Higgins, *et al.*, 2015 *Arabidopsis*
718 PCH2 mediates meiotic chromosome remodeling and maturation of crossovers. *PLOS Genet.*
719 11: 1–27.
720
721 Longair, M. H., D. A. Baker, and J. D. Armstrong, 2011 Simple neurite tracer: Open source
722 software for reconstruction, visualization and analysis of neuronal processes. *Bioinformatics*
723 27: 2453–2454.
724
725 Lynn, A., K. E. Koehler, L. Judis, E. R. Chan, J. P. Cherry, *et al.*, 2002 Covariation of
726 synaptonemal complex length and mammalian meiotic exchange rates. *Science* 296: 2222–
727 2225.
728
729 Lynn, A., R. Soucek, and G. V. Börner, 2007 ZMM proteins during meiosis: Crossover
730 artists at work. *Chromosom. Res.* 15: 591–605.
731
732 Mercier, R., S. Jolivet, D. Vezon, E. Huppe, L. Chelysheva, *et al.*, 2005 Two meiotic
733 crossover classes cohabit in *Arabidopsis*: One is dependent on MER3, whereas the other one
734 is not. *Curr. Biol.* 15: 692–701.
735
736 Mercier, R., C. Mezard, E. Jenczewski, N. Macaisne, and M. Grelon, 2014 The molecular
737 biology of meiosis in plants. *Annu. Rev. Plant Biol.* 66: 1–31.
738
739 Modliszewski, J. L., and G. P. Copenhaver, 2015 Meiotic recombination heats up. *New*
740 *Phytol.* 208: 295–297.
741
742 Molnar, M., J. Bahler, M. Sipiczki, and J. Kohli, 1995 The *rec8* gene of
743 *Schizosaccharomyces pombe* is involved in linear element formation, chromosome pairing
744 and sister-chromatid cohesion during meiosis. *Genetics* 141: 61–73.
745

746 Morgan, C. H., H. Zhang, and K. Bomblies, 2017 Are the effects of elevated temperature on
747 meiotic recombination and thermotolerance linked via the axis and synaptonemal complex?
748 Philos. Trans. R. Soc. Lond. B. Biol. Sci. 372: 20160470.
749

750 Otto, S., 2009 The evolutionary enigma of sex. Am. Nat. 174: S1–S14.
751

752 Pecinka, A., H. Q. Dinh, T. Baubec, M. Rosa, N. Lettner, *et al.*, 2010 Epigenetic regulation
753 of repetitive elements is attenuated by prolonged heat stress in *Arabidopsis*. Plant Cell 22:
754 3118–29.
755

756 Perkins, A. T., T. M. Das, L. C. Panzera, and S. E. Bickel, 2016 Oxidative stress in oocytes
757 during midprophase induces premature loss of cohesion and chromosome segregation errors.
758 Proc. Natl. Acad. Sci. U. S. A. 113: E6823–E6830.
759

760 Phillips, D., G. Jenkins, M. Macaulay, C. Nibau, J. Wnetrzak, *et al.*, 2015 The effect of
761 temperature on the male and female recombination landscape of barley. New Phytol. 208:
762 421–429.
763

764 Plough, H. H., 1917 The effect of temperature on crossingover in *Drosophila*. J. Exp. Zool.
765 24: 147–209.
766

767 Presgraves, D. C., 2005 Recombination enhances protein adaptation in *Drosophila*
768 *melanogaster*. Curr. Biol. 15: 1651–1656.
769

770 Rees, H., and J. Thompson, 1958 Genotypic control of chromosome behaviour in rye V. The
771 distribution pattern of chiasmata between pollen mother cells. Heredity 12: 101–111.
772

773 Ritz, K. R., M. A. F. Noor, and N. D. Singh, 2017 Variation in recombination rate: Adaptive
774 or not? Trends Genet. 33: 364–374.
775

776 Rog, O., Kohler, S., and A. F. Dernburg, 2017 The synaptonemal complex has liquid
777 crystalline properties and spatially regulates meiotic recombination factors. Elife 6: e21455.
778

779 Ross-Ibarra, J., 2004 The evolution of recombination under domestication: A Test of two
780 hypotheses. Am. Nat. 163: 105–112.
781

782 Saleem, M., B. Lamb, and E. Nevo, 2001 Inherited differences in crossing over and gene
783 conversion frequencies between wild strains of *Sordaria fimicola* from “Evolution Canyon.”
784 Genetics 159: 1573–1593.
785

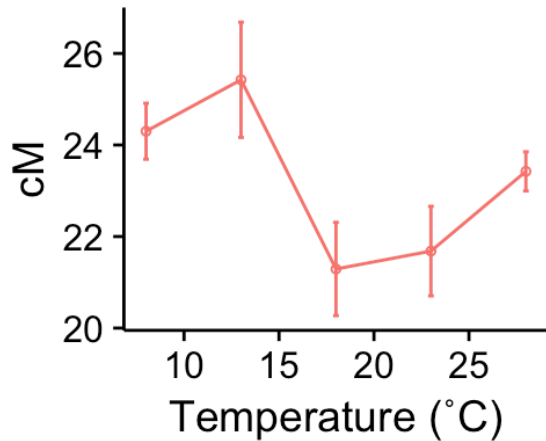
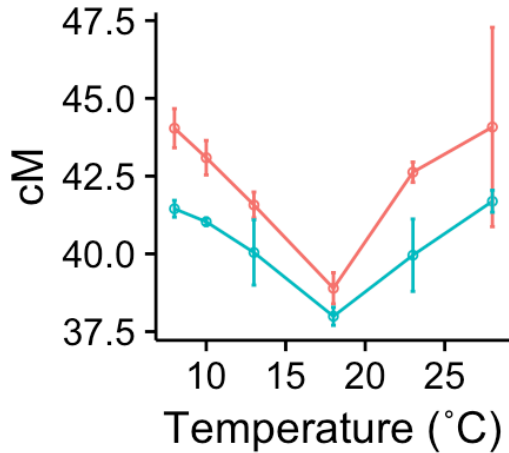
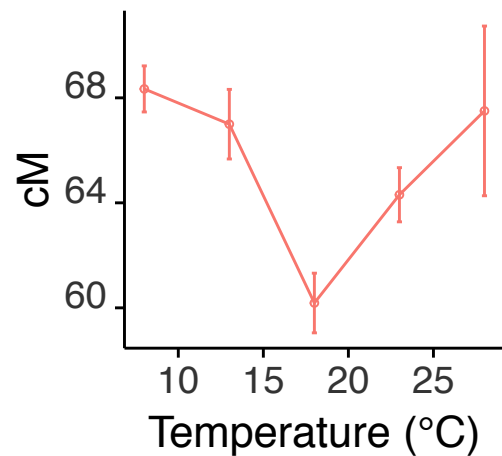
786 Shaw, D., 1971 Genetic and environmental components of chiasma control. I. Spatial and
787 temporal variation in *Schistocerca* and *Stethophyma*. Chromosoma 34: 281–301.
788

789 Smith, H. F., 1936 Influence of temperature on crossing-over in *Drosophila*. Nature 138:
790 329–330.
791

792 Stern, C., 1926 An effect of temperature and age on crossing-over in the first chromosome of
793 *Drosophila melanogaster*. Proc. Natl. Acad. Sci. U. S. A. 12: 530–532.
794

795 Stern, H., 1986 Meiosis: Some considerations. J. Cell Sci. Suppl. 4: 29–43.

796
797 Turner, T. L., M. T. Levine, M. L. Eckert, and D. J. Begun, 2008 Genomic analysis of
798 adaptive differentiation in *Drosophila melanogaster*. *Genetics* 179: 455–473.
799
800 White, M. A., S. Wang, L. Zhang, and N. Kleckner, 2017 Quantitative modeling and
801 automated analysis of meiotic recombination, pp. 305-323 in *Meiosis*, edited by D. T. Stuart.
802 Springer, New York.
803
804 Wilson, J. Y., 1959 Chiasma frequency in relation to temperature. *Genetica* 29: 290–303.
805
806 Wright, K. M., B. Arnold, K. Xue, M. Šurinová, J. O'Connell, *et al.*, 2015 Selection on
807 meiosis genes in diploid and tetraploid *Arabidopsis arenosa*. *Mol. Biol. Evol.* 32: 944–955.
808
809 Yelina, N. E., P. A. Ziolkowski, N. Miller, X. Zhao, K. A. Kelly, *et al.*, 2013 High-
810 throughput analysis of meiotic crossover frequency and interference via flow cytometry of
811 fluorescent pollen in *Arabidopsis thaliana*. *Nat. Protoc.* 8: 2119–2134.
812
813 Yin, H., X. Zhang, J. Liu, Y. Wang, J. He, *et al.*, 2009 Epigenetic regulation, somatic
814 homologous recombination, and abscisic acid signaling are influenced by DNA polymerase
815 epsilon mutation in *Arabidopsis*. *Plant Cell* 21: 386–402.
816
817 Zhang, L., Z. Liang, J. Hutchinson, and N. Kleckner, 2014 Crossover patterning by the beam-
818 film model: analysis and implications. *PLoS Genet.* 10: e1004042.
819
820 Zickler, D., and N. Kleckner, 1999 Meiotic chromosomes: Integrating structure and function.
821 *Annu. Rev. Genet.* 33: 603–754.
822
823 Zickler, D., and N. Kleckner, 2015 Recombination, pairing, and synapsis of homologs
824 during meiosis. *Cold Spring Harb. Perspect. Biol.* 7: a016626.
825
826 Ziolkowski, P. A., C. J. Underwood, C. Lambing, M. Martinez-Garcia, E. J. Lawrence, *et al.*,
827 2017 Natural variation and dosage of the HEI10 meiotic E3 ligase control *Arabidopsis*
828 crossover recombination. *Genes Dev.* 31: 306–317.

A**I3bc****B****I5ab****C****I3ab + I5ab**

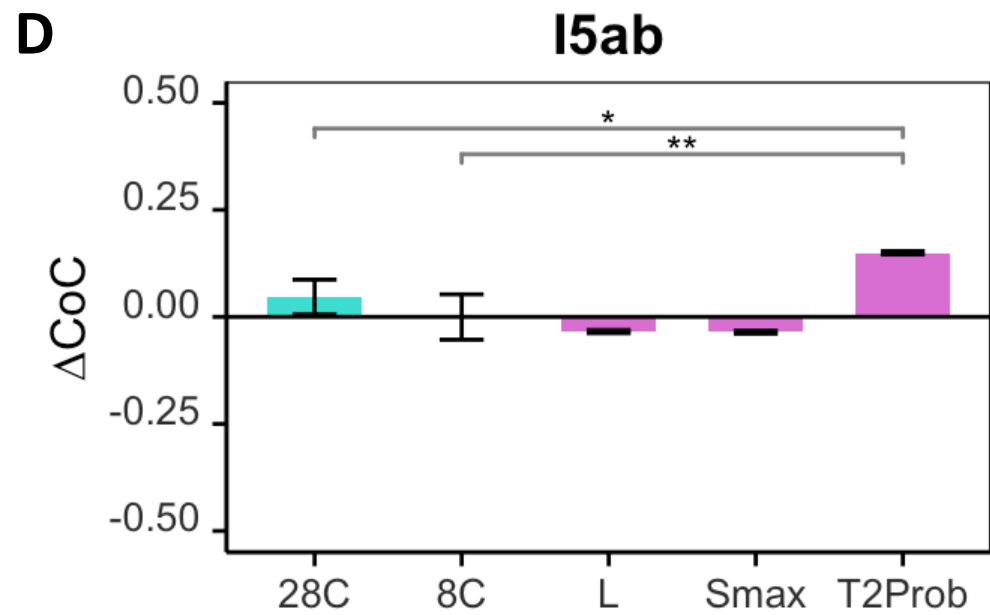
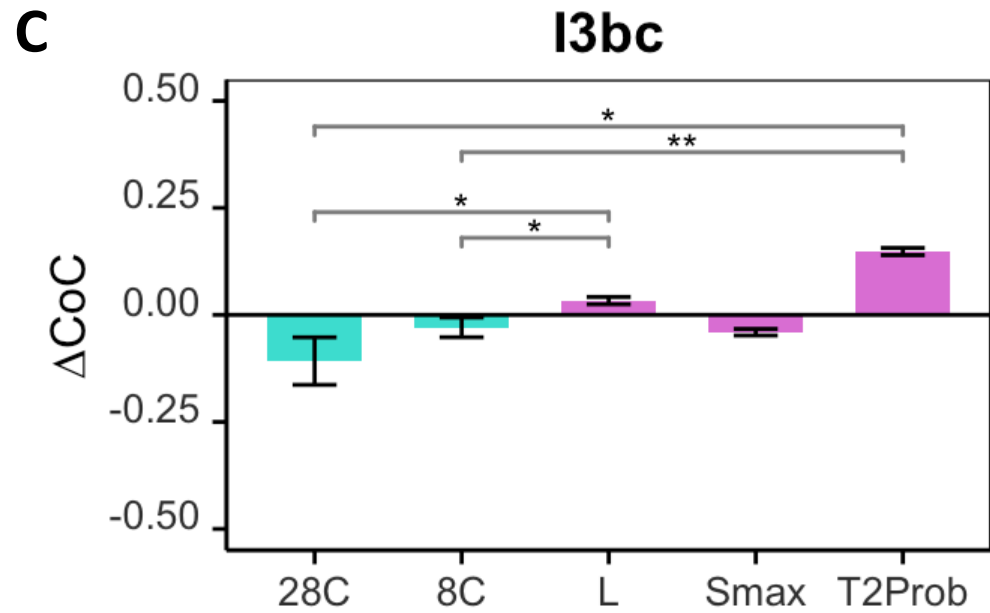
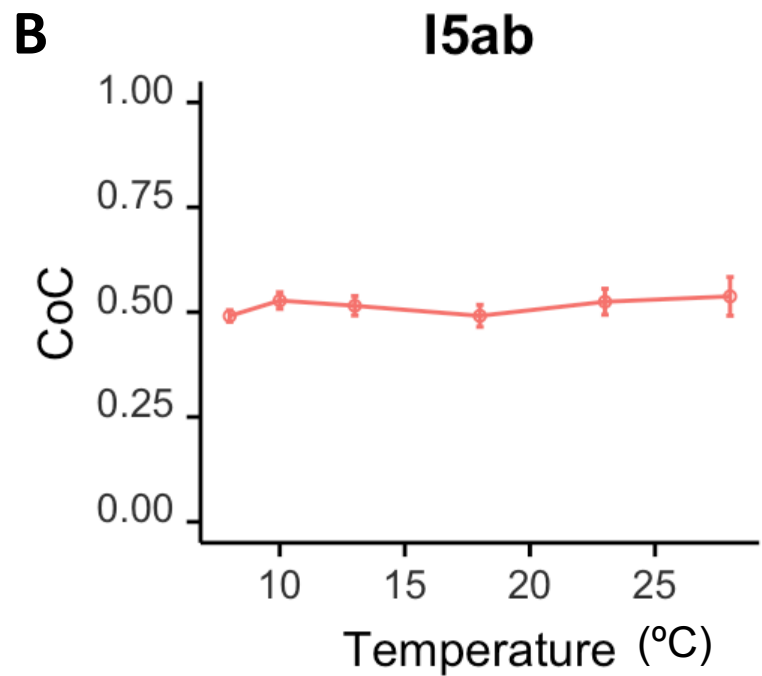
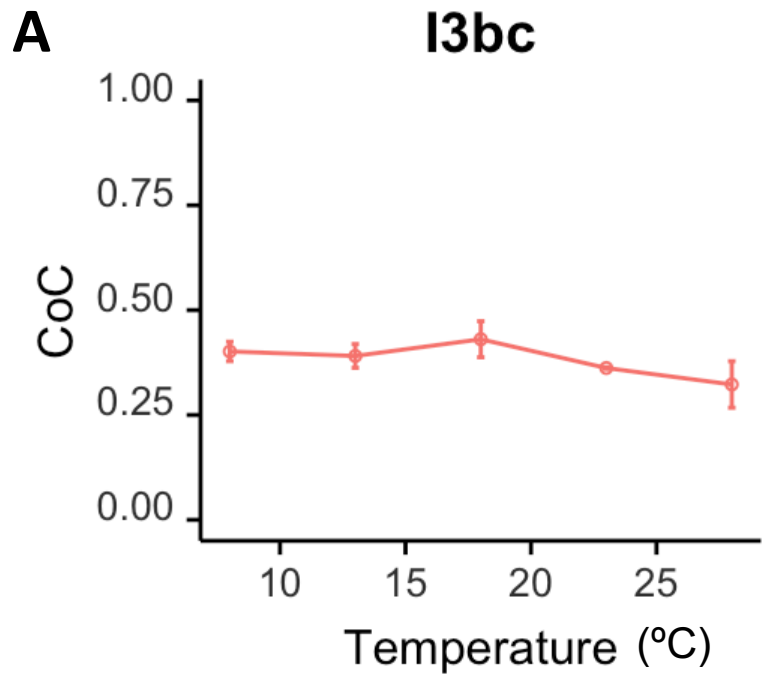


Table 1. Best-fit parameters* for chromosomes 3 and 5

Chr	N	B	E	Bs	Be	Bd	Smax	Bsmax	A	L	cL	cR	M	T2prob
														0.0095
5	56	1	0.6	0.4	0.5	0.01	4.5 (15)	1	1	1 (0.54)	0.8	1.05	1	(0.0155)
										0.9				0.01
3	49	1	0.6	0.5	0.65	0.01	1 (2.03)	1	1	(0.641)	1.5	1.5	1	(0.0162)

*whole chromosomes were simulated, with best-fit parameters based on FTL derived CO and CoC values

Values in brackets are those used to achieve a 13% increase in COs